

# **UCLA**

## **Earthquake Engineering**

### **Title**

Kinematic soil-structure interaction effects from building and free-field seismic arrays in Japan

### **Permalink**

<https://escholarship.org/uc/item/8mk017th>

### **Authors**

Givens, Michael J  
Mikami, Atsushi  
Kashima, Toshihide  
[et al.](#)

### **Publication Date**

2012-03-06

### **License**

[CC BY 4.0](#)

## KINEMATIC SOIL-STRUCTURE INTERACTION EFFECTS FROM BUILDING AND FREE-FIELD SEISMIC ARRAYS IN JAPAN

Michael J. Givens<sup>1)</sup>, Atsushi Mikami<sup>2)</sup>, Toshihide Kashima<sup>3)</sup>, and Jonathan P. Stewart<sup>1)</sup>

1) Department of Civil & Environmental Engineering, University of California, Los Angeles, United States

2) Department of Civil & Environmental Engineering, The University of Tokushima, Japan

3) International Institute of Seismology and Earthquake Engineering, Building Research Institute, Japan

mjgivens@gmail.com, amikami@ce.tokushima-u.ac.jp, kashima@kenken.go.jp, jstewart@seas.ucla.edu

**Abstract:** Ground motions at the foundation levels of structures differ from those in the free-field as a result of inertial and kinematic interaction effects. Inertial interaction effects tend to produce narrow-banded ground motion modification near the fundamental period of the soil-structure system, whereas kinematic effects are relatively broad-banded and concentrated at high frequencies. Kinematic interaction effects can be predicted using relatively costly finite element analyses with incoherent input or simplified models. The simplified models are semi-empirical in nature and derived from California data. These simplified models are the basis for seismic design guidelines used in the western United States, such as ASCE-41 and a pending report published by NIST. We compile some available data from building and ground instrumentation arrays in Japan for comparison to these two sets of models. We demonstrate that the model predictions for the sites under consideration are very similar to each other for modest foundation sizes (equivalent radii under about 50 m). However, the data show that both approaches overestimate the transfer function ordinates relative to those from Japanese data. This indicates that the semi-empirical models currently in use are conservative relative to these data sets. We speculate as to possible causes for the observed discrepancies.

### 1. INTRODUCTION

Foundation-level and free-field seismic ground motions are identical only for vertically propagating incident waves and non-embedded foundations. In reality, incident waves are neither vertically propagating nor coherent, which gives rise to spatially variable ground motions even on sites with relatively uniform site conditions. In the presence of such incident wave fields, motions on foundations will be reduced in amplitude relative to free-field motions, an effect termed *base slab averaging*. Base slab averaging is one type of *kinematic soil-structure interaction* effect. Other kinematic effects result from foundation embedment below the ground surface (e.g., buildings with basements) and the presence of pile foundations.

The spatial variability of seismic ground motions in the free-field (i.e., away from building foundations), has been examined by a number of investigators (e.g., Abrahamson, 1991; Zerva and Zervas, 2002) who have derived empirical functions that express the variability of phase angle in terms of a coherency function. Those functions were derived largely using dense array records from Lotung, Taiwan, although they have since been validated and adjusted using data from other arrays (Ancheta et al., 2011). Recently, Abrahamson's ground motion coherency model was implemented into the Computer Program SASSI (a System for Analysis of Soil-Structure Interaction; Ostadan, 2005). SASSI computes the relative motion of the foundation to the free-field (input motion) in terms of a transfer function expressing the frequency-dependent ratio of foundation motion amplitude to free-field motion amplitude. The result is one solution to the kinematic interaction problem, including base slab

averaging.

Another approach that has been utilized to predict foundation/free-field transfer functions from base slab averaging is based on a theoretical solution by Veletsos and co-workers (1989, 1997) coupled with empirical calibration of an incoherence parameter by Kim and Stewart (2003). This approach is inherently calibrated for California sites, but the degree to which its application is appropriate for building types not represented in the database and regions other than California remains unknown. This approach has been implemented for engineering application, in combination with a simple transfer function for embedment effects, in two design standards: ASCE-41 and NIST (NEHRP CJV, 2012).

In this paper, we apply the above two models for predicting transfer functions to a subset of the available data from Japan for several particularly interesting structures. Both models are applied under the assumption of vertically propagating, incoherent incident wave fields, with the implicit understanding that bias could result from this assumption under some circumstances. The predicted transfer functions are compared to each other and to transfer functions derived from the data.

### 2. STRUCTURAL-GROUND ARRAYS IN JAPAN

As part of an ongoing project, we compiled a list of instrumented structures in Japan with neighboring ground stations, which can be used for the evaluation of foundation/free-field ground motion variations of the type described in the *Introduction*. This list of structures is given in Table 1.

Table 1. List of currently compiled instrumented structure and ground arrays in Japan.

Location	Array owner	Lat/Long	Station code	Two base vertical sensors (Y/N)	# Stories above ground	# Basement levels	Foundation type	Instrumented stories	Site condition	# Earthquakes recorded
Sendai, Miyagi	Tohoku Institute of Technology	38°14'44"N, 140°51'12"E	J1	no	4	0	pile	GL,4,FF		100
Hachinohe, Aomori	Hachinone National College of Tech.	40°29'32"N, 141°26'57"E	J5	no		0	pile	GL,FF		
Toda Corp., Tsukuba?	Toda Corporation	36°06'37"N, 140°04'36"E	J6		6	0	pile	GL,6,FF		13
Tokushima Univ.	The University of Tokushima	34°04'39"N, 134°33'46"E	J7	no	6	0	pile	GL,6,FF	sand	2
Nihon Univ. Bldg. #14	Nihon University	35°43'31"N, 140°03'28"E			5	1	pile	GL,4,RF,FF		many
Nagoya Univ.	Nagoya University	35°09'20"N, 136°58'01"E								
	Hachinohe Institute of Technology	40°28'44"N, 141°33'36"E								
		35°00'45"N, 135°46'06"E			7	1		B1,7,4,FF		
	Nikken Sekkei	35°41'59"N, 139°45'04"E								
	Shimizu Corporation	35°39'46"N, 139°47'52"E								
	Kanagawa University	35°29'07"N, 139°37'13"E			8	2		B2,B1,3,6,8		
<b>NPS</b>										
NPS Kashiwazaki	Tokyo Electric Power Company	37°25'17"N, 138°35'44"E								
NPS Fukushima	Tokyo Electric Power Company	37°25'14"N, 141°01'59"E								
NPS Onagawa	Tohoku Electric Power Company	38°24'04"N, 141°29'59"E								
<b>BRI</b>										
Takamatsu, Kagawa	BRI	34°20'20"N, 134°02'48"E	J2, TKM	no	8	1	pile?	B1,RF,FF	sand	23
Fukuoka, Fukuoka	BRI	33°35'16"N, 130°25'27"E	J3	no	10	1	pile	B1,10,FF	sand	14
Nagoya, Aichi	BRI	35°10'51"N, 136°54'11"E	J4, FKO	no	12	2	pile	B2,GL,12	sand	55
Miyako	BRI	39°38'29"N, 141°57'25"E	MYK		7	0		GL,7,FF		224
Hachinohe	BRI	40°30'42"N, 141°29'20"E	HCN2		10	1		B1, GL,10,FF		467
Yachiyo	BRI	35°43'20"N, 140°05'59"E	YCY		6	1		B1,GL,7		23
Nippon Inst. Tech.	BRI	36°01'38"N, 139°42'41"E	NIT		6	1		GL,6,FF		327
Misato City Hall	BRI	35°49'48"N, 139°52'20"E	MST	no	7	1		GL,7,FF		14
Funabashi	BRI	35°42'26"N, 140°00'20"E	FNB		8	0		GL,8,FF		37
Chiba	BRI	35°36'24"N, 140°07'22"E	CHB		8	1		B1,GL,8		23
Toda City Hall	BRI	35°49'03"N, 139°40'40"E	TDS		8	1		B1,GL,8		27
The National Museum of Western Art	BRI	35°42'55"N, 139°46'32"E	NMW		3	1		B1,GL,4,FF		264
Univ. of Tokyo, Bldg.11	BRI	35°42'49"N, 139°45'34"E	UTK		9	0		GL,7,FF		49
Marine Sci. and Tech.	BRI	35°37'42"N, 139°44'53"E	TUF		7	0		GL,7,FF		37
College of MLIT	BRI	35°43'08"N, 139°28'53"E	KDI		3	0		GL,3,FF		69
Yamanashi Pref. Hall	BRI	35°39'50"N, 138°34'06"E	YMN		8	1		B1,GL,8,FF		15
Kushiro	BRI	42°59'11"N, 144°22'40"E	KGC		9	1		B1,GL,9,FF		253
Olumpic	BRI	35°40'36"N, 139°41'39"E	YYG		4	1		B1,GL,4		16
	BRI	36°07'58"N, 140°04'34"E	NCTD		7	0		GL,8,FF		2
	BRI	35°40'42"N, 139°44'39"E	NDLM		5	4		GL,17		48
	BRI	35°40'44"N, 139°44'38"E	NDLA		4	8		B8,B4,GL,4		37
	BRI	35°40'41"N, 139°44'42"E	NDLG							242
	BRI	36°07'55"N, 140°04'24"E	ANX		8	1		B1,GL,2,5,8,FF, ground array		1142

B# = Basement floor level #, BRI = Building Research Institute, FF = Free-field, GL = Ground level, Ground array = sensors at depth in soil, NPS = Nuclear power station, and RF = Roof level

The Building Research Institute (BRI) in Japan owns most of the structural-ground arrays and distributes seismic data at the web site: <http://smo.kenken.go.jp/>. Most of the BRI instrumented buildings range from 3 to 10 stories in height above ground. Foundation types are not provided on the site. Base rocking cannot be directly estimated for most of these buildings since BRI sensor array configurations typically have only one vertical accelerometer at its lowest level.

The Electric Power Company in Japan is another major owner of structural-ground arrays from in nuclear power stations. When released for public use, the data is distributed by the Japan Association for Earthquake Engineering (JAE) at their web site: <http://www.jae.gr.jp/stack/sta05.html>.

From the list in Table 1, we select three buildings for consideration in this manuscript: Nagoya office building (hereafter referred to as ‘Nagoya’), Onagawa nuclear power plant (‘Onagawa’), and Sendai university building (‘Sendai’).

The Sendai site consists of a four story building above ground and contains nine accelerometers (including three free-field), as shown in Figure 1. Lateral loads are resisted by reinforced concrete frames and shear walls in the longitudinal and transverse directions, respectively. The foundation consists of end-bearing concrete piles connected by grade beams. Figure 1 shows the underlying soil stratigraphy and geophysical data that were determined from boring operations which included suspension logging at the site (OYO Corporation, 2007). The Sendai site was investigated previously by Mikami et al. (2006) using data from the 2003 Off Miyagi earthquake. This data is considered again here along with recordings from the recent 2011 Tohoku earthquake, which produced much stronger ground motions. The site peak ground acceleration (PGA) for the Off Miyagi and Tohoku earthquakes are 0.232g and 0.813g, respectively. The purpose for selecting this site was to examine possible differences in the kinematic response for the variable strengths of shaking.

The Onagawa site consists of a five story reactor above ground with two sub-terranean levels (embedment of 16 m) and contains 22 accelerometers (including three free-field), as shown in Figure 2. The foundation consists of a 3.5 m thick concrete slab with dimensions of 55.3 by 51.8 m. Figure 2 shows the underlying soil lithology and geotechnical data. The Onagawa structure was selected because it has the only available array that enables evaluation of base rocking. The site is investigated for the 2011 Tohoku earthquake that had a PGA of 0.533g at the site.

The Nagoya site consists of a 10 story building above ground with two basement levels (embedment of 12.83 m) and contains 9 accelerometers (including three free-field), as shown in Figure 3. The foundation consists of a 2.53 m thick concrete slab with dimensions of 79.6 by 23.2 m overlying reinforced concrete piles. Figure 3 shows the underlying soil lithology and geotechnical data that were determined from boring operations which included suspension logging 440 m west of the site (CRBOMLIT, 2003). The Nagoya structure was selected because it has a large footprint area, which is of interest because its dimensions are near the limit of the calibration range for the Kim and Stewart (2003) semi-empirical model. The site was investigated for the 2004 Off Kii Peninsula earthquake that had a PGA of 0.014g. To our knowledge, neither the Onagawa nor

the Nagoya structures have been examined in prior studies.

### 3. MODELS FOR PREDICTION OF FOUNDATION TO FREE-FIELD TRANSFER FUNCTIONS

#### 3.1 Spatial Coherency Model Implemented in SASSI

The spatial variation of phase of strong ground motion is quantified by coherency. Using recordings from dense arrays in Lotung, Taiwan Abrahamson (1991) derived empirical functions that describe coherency as a function of separation distance and frequency. Coherency is unity at zero frequency and reduces strongly with increasing frequency and relatively weakly with increasing distance. Coherency less than unity results both from deterministic phase lag and relatively random (stochastic) wave scattering effects. Abrahamson (1991) present a model for *lagged coherency*, which represents the stochastic component only (wave passage removed). The model is considered applicable to frequencies greater than 1 Hz and for separation distances of 6 to 85 meters (Abrahamson, 1991). That coherency model has been implemented into SASSI by Ostadan (2005) and ACS-SASSI by Ghiocel (2006).

SASSI was originally developed at the University of California, Berkeley (Lysmer et al., 1981, 1999). SASSI utilizes the substructuring approach in which the linear SSI problem is divided into sub problems based on the principle of superposition; thus the analysis is performed using linear material properties. Soil is assumed to consist of horizontal layers overlying either a rigid base or an elastic half-space. The structure and foundation are modeled by finite elements. Foundations are modeled as rigid, massless slabs to exclude inertial effects. Piles are modeled as hollow elements using representative stiffness of prestressed high-strength concrete.

#### 3.2 Semi-Empirical Approach

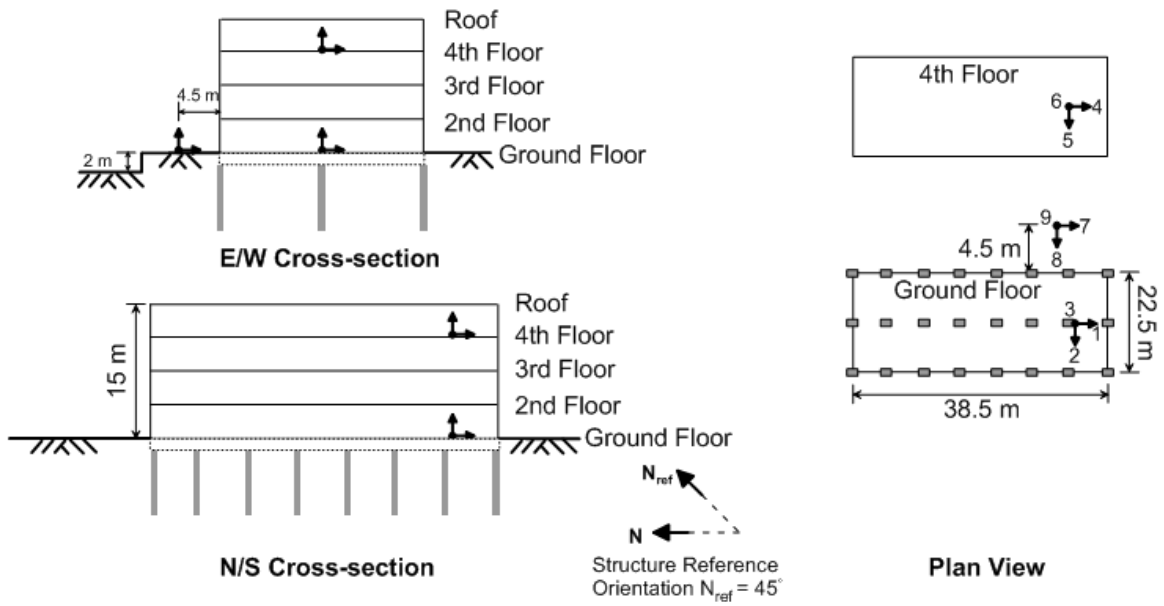
Veletsos and co-workers (1989, 1997) developed useful models for theoretical base slab averaging that combine an analytical representation of the spatial variation of ground motion with rigorous treatment of foundation-soil contact.

Kim and Stewart (2003) calibrated Veletsos’ analysis procedure against observed foundation/free-field ground motion variations as quantified by frequency dependent transfer functions. Two types of transfer functions can be obtained from well instrumented structures as follows:

$$H_u(\omega) = \frac{u_f}{u_g} \quad H_\theta = \frac{\theta L}{u_g} \quad (1)$$

where  $u_f$  denotes foundation translation,  $u_g$  ground motion translation in the same direction,  $\theta$  denotes kinematic rotation about an axis normal to the direction of  $u_f$  and  $u_g$ , and  $L$  is the foundation half dimension in the same direction as  $u_f$  and  $u_g$ . The Kim and Stewart calibration considered the horizontal translation transfer function only ( $H_u$ ), and resulted in apparent  $\kappa$  values (denoted  $\kappa_d$ ) for each structure/data set combination. Those  $\kappa_d$  values reflect not only incoherence effects, but necessarily also include average foundation flexibility and wave inclination effects for the calibration data set.

### Sensor Array Location Map



### Soil Properties

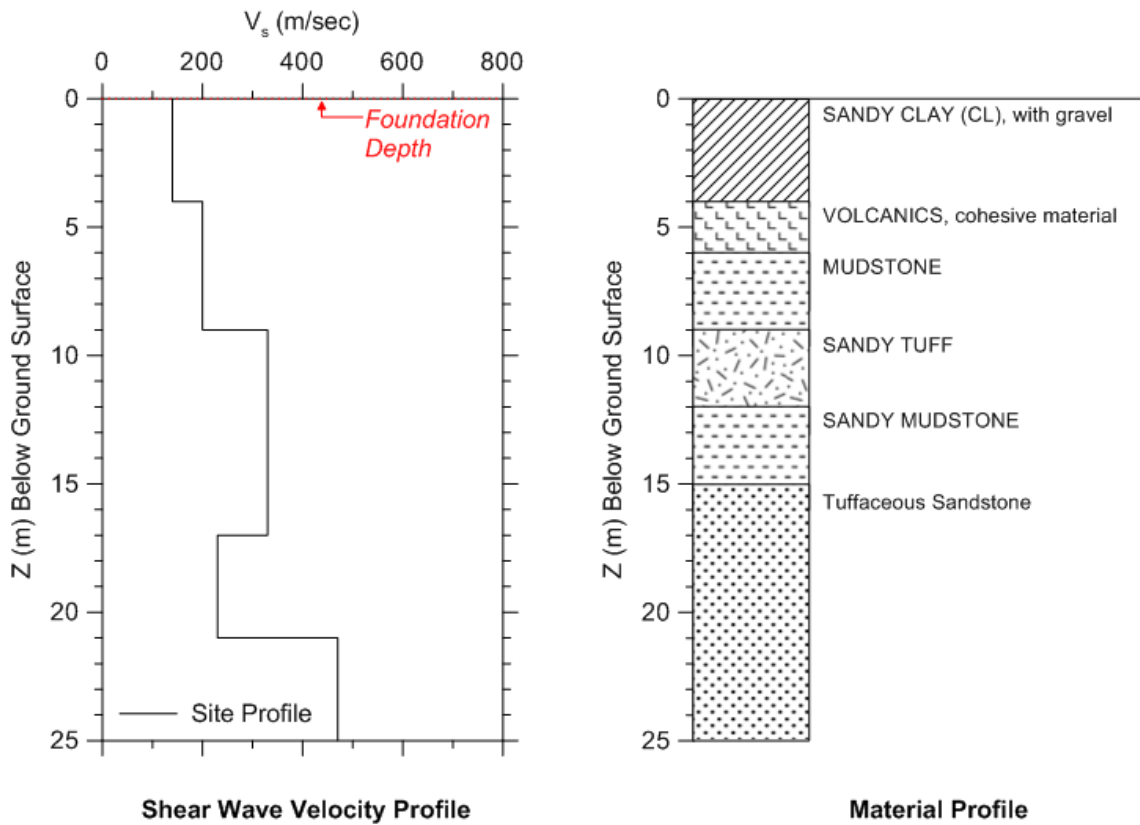
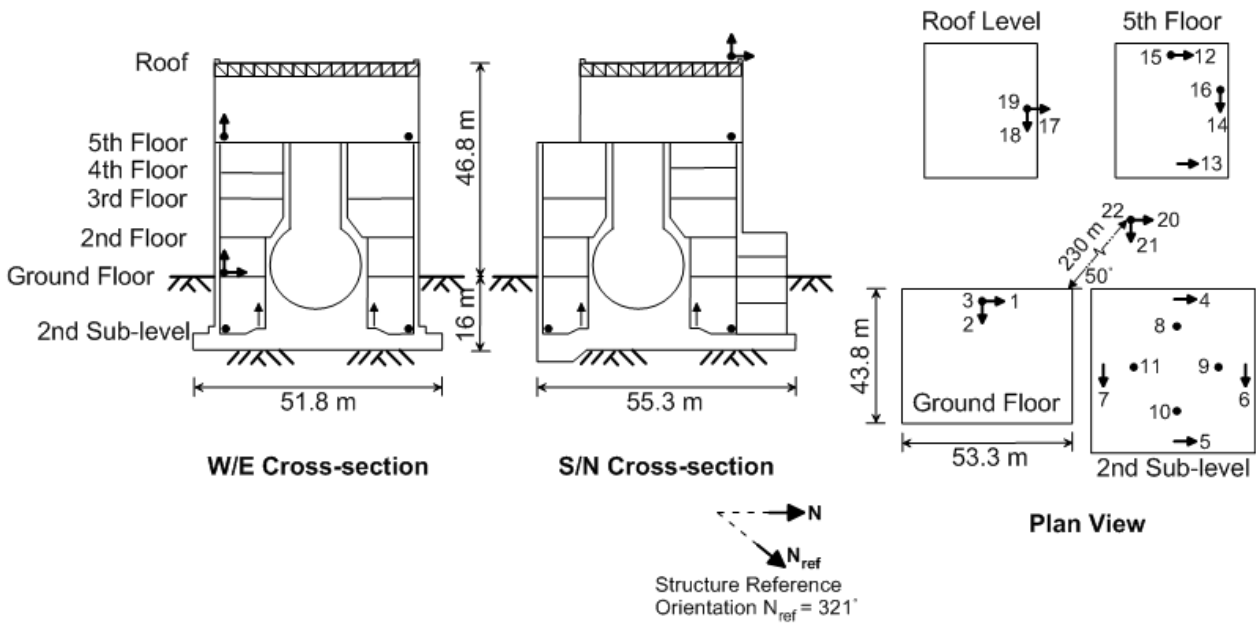


Figure 1. Building layout and site conditions at Sendai University site (J1). Data source: OYO Corporation, 2007.

### Sensor Array Location Map



### Soil Properties

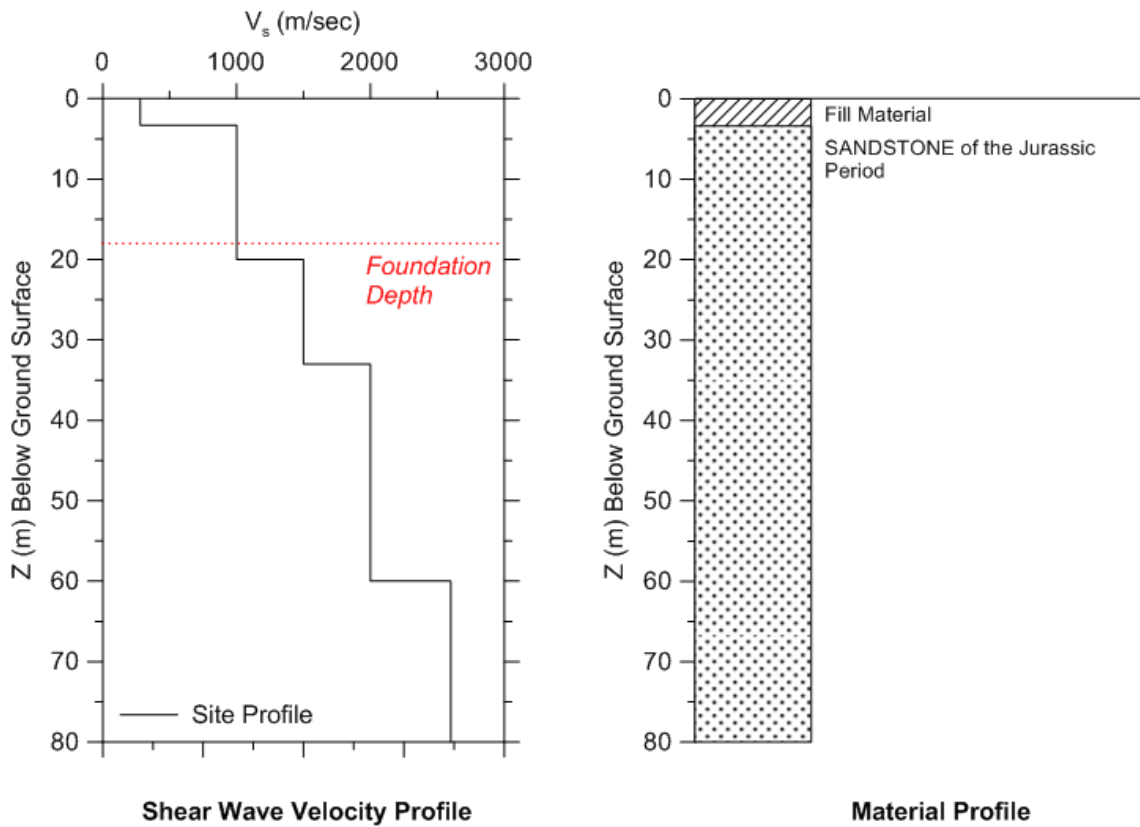
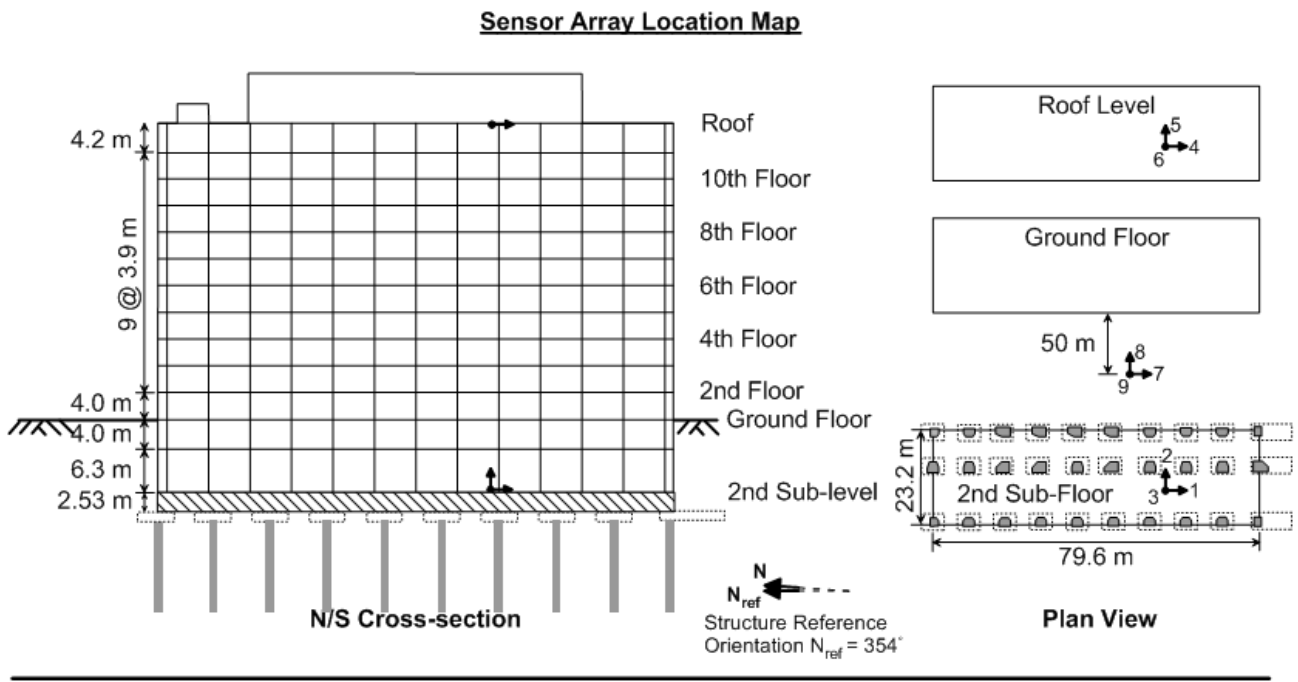


Figure 2. Building layout and site conditions at Onagawa Nuclear Power Plant, Reactor 1. Data sources: Tohoku Electric Power Company, 2009 and 2011.



### Soil Properties

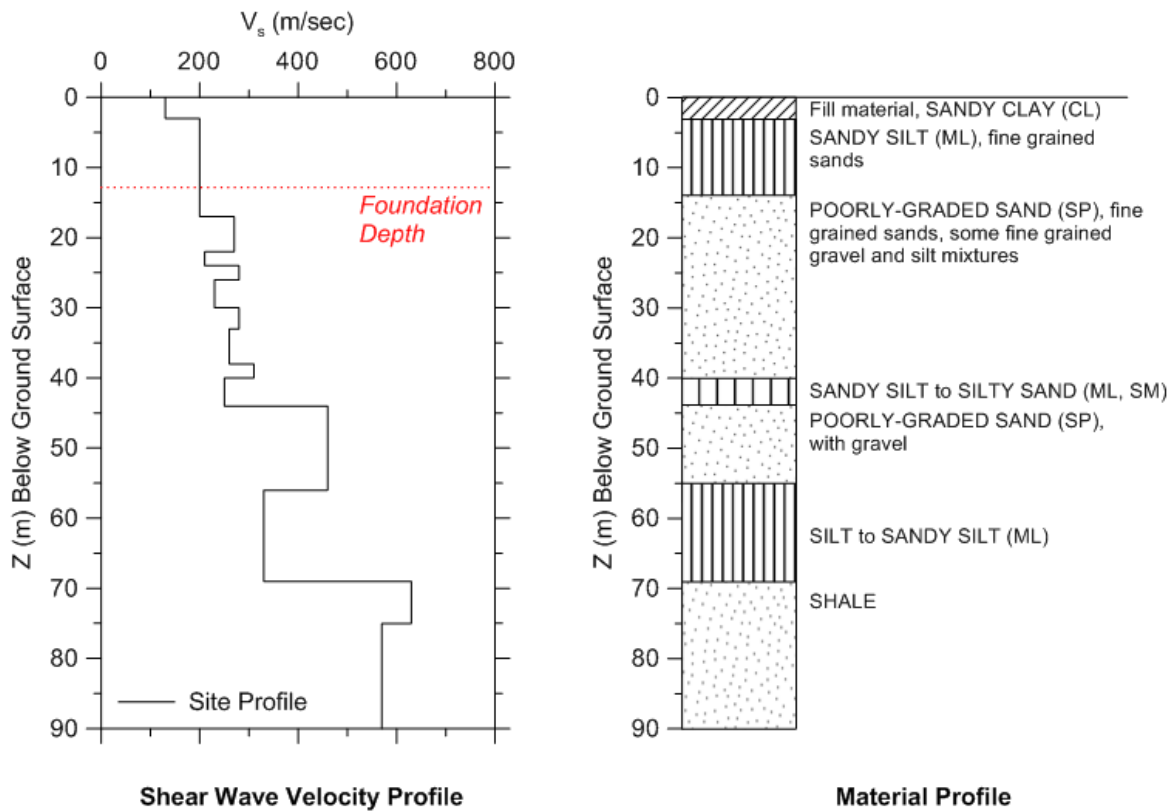


Figure 3. Building layout and site conditions at Nagoya Office Building (J4). Data sources: CRBOMLIT, 2003 and 2005.

The data set considered by Kim and Stewart (2003) consisted of buildings with mat, footing and grade beam, and grade beam and friction pile foundations, generally with base dimensions in the range of  $B_e^A=15-40$  m (where  $B_e^A$  is the square root of foundation area divided by four). Although the Veletsos models strictly apply to rigid foundations, the semi-empirical model applies to the more realistic foundation conditions present in the calibration data set, which consist principally of shallow foundations that are inter-connected (i.e., continuous mats or footings interconnected with grade beams). Errors could occur when the model is applied to conditions beyond the calibration data set. In particular, the effects of incoherence in the Veletsos models is taken as proportional to wavelength, thus implying strong scaling with frequency and distance. As mentioned previously, array data indicates the distance scaling is much weaker than the frequency scaling (Abrahamson et al., 1991; Ancheta et al., 2011), so the model would be expected to over-predict the effects of incoherence (under-predict  $H_u$ ) for very large foundations (opposite for small foundations). Even within the parameter space of the calibration data set, it should be recognized that the empirical model fits the data set in an average sense but would not be expected to match any particular observation. Example applications showing fits to data are given in subsequently in the paper.

Two of the three buildings considered in this research have foundation embedment (Nagoya and Onagawa). We utilize a model originally presented by Kausel et al. (1978) in combination with the Kim and Stewart model for these buildings. As presented by NIST (NEHRP CJV, 2012), the model is given as follows:

$$H_u = \cos\left(\frac{D\omega}{V_s}\right), \quad \frac{D\omega}{V_s} < 1.1 \quad (2a)$$

$$H_u = 0.45, \quad \frac{D\omega}{V_s} > 1.1 \quad (2b)$$

$$H_\theta(\omega) = 0.26\left(1 - \cos\left(\frac{D\omega}{V_s}\right)\right), \quad \frac{D\omega}{V_s} < \frac{\pi}{2} \quad (3a)$$

$$H_\theta(\omega) = 0.26, \quad \frac{D\omega}{V_s} > \frac{\pi}{2} \quad (3b)$$

where  $D$  = embedment depth and  $V_s$  is a time-averaged shear wave velocity over the embedment depth of the foundation.

## 4. EVALUATION AND COMPARISON OF TRANSFER FUNCTIONS

### 4.1 Transfer Function Calculation from Data

Transfer functions are evaluated from the recordings using procedures described in Mikami et al. (2008). In particular, frequency domain smoothing is applied to spectral density functions for the ‘input’ (denominator in Eq. 1, denoted  $y$ ) and ‘output’ (numerator in Eq. 1, denoted  $x$ ) as follows:

$$|H(\omega)| = \sqrt{\frac{S_{xx}}{S_{yy}}} \quad (4)$$

where  $S_{xx}$  and  $S_{yy}$  are auto-spectral density functions for the input and output, respectively. The smoothing is applied using an 7-point Hamming window, which provides an equivalent frequency bandwidth of  $B_e = 0.207$  Hz. In addition, the coherence (square of coherency) of the data is calculated as:

$$\gamma^2(\omega) = \frac{|S_{xy}(\omega)|^2}{S_{xx}(\omega)S_{yy}(\omega)} \quad (5)$$

where  $S_{xy}$  is the cross spectral density function. The coherence is used to judge the effects of noise in the data. Frequency ranges in the transfer function that are dominated by noise will have low coherence. The average coherence of pairs of white noise signals for our frequency bandwidth is  $0.25 \pm 0.04$  (Mikami et al., 2008).

### 4.2 Application of Models

The models described in Section 3 are applied to the conditions at the three building sites. Equivalent linear shear wave velocity profiles were developed using deconvolution analysis with the free-field ground motions and velocity profiles shown in Figures 1-3. Nonlinear properties were developed based on the soil conditions using the modulus reduction and damping models from Menq (2003) for sands and Darendeli (2001) for other soil and weathered rock materials.

The properties developed through the above process are the direct input for the SASSI analysis, which is a linear analysis with no iteration on strain-dependent soil properties. The model for embedment used a time-averaged version of these velocities over the embedment depth for use in Eqs. 2-3. The Kim and Stewart model also uses a shear wave velocity for the evaluation of the  $\kappa_a$  parameter, which is time-averaged over the depth range zero to  $D+B_e^A$ .

### 4.3 Results for Subject Buildings

Figures 4–8 show predicted transfer functions from the SASSI and NIST models along with transfer function and coherence ordinates for each site considered. The dots show transfer function ordinates with high coherence.

The predicted transfer function ordinates are similar from the SASSI and NIST models for each considered structure. Further research is needed to evaluate the range of foundation conditions where this similarity holds.

Figures 4-5 present results for the Sendai site for the two earthquakes. The transfer and coherence functions from the two sets of earthquake recordings are remarkably similar for the two events. For frequencies less than about 8 Hz where the data have high coherence and hence relatively little effects of noise, the transfer functions are nearly identical. The transfer functions from data fall below those from the two models to a significant degree for frequencies beyond 2.5 Hz. This occurs despite the slower velocities produced by the larger shear strains in the Tohoku earthquake.



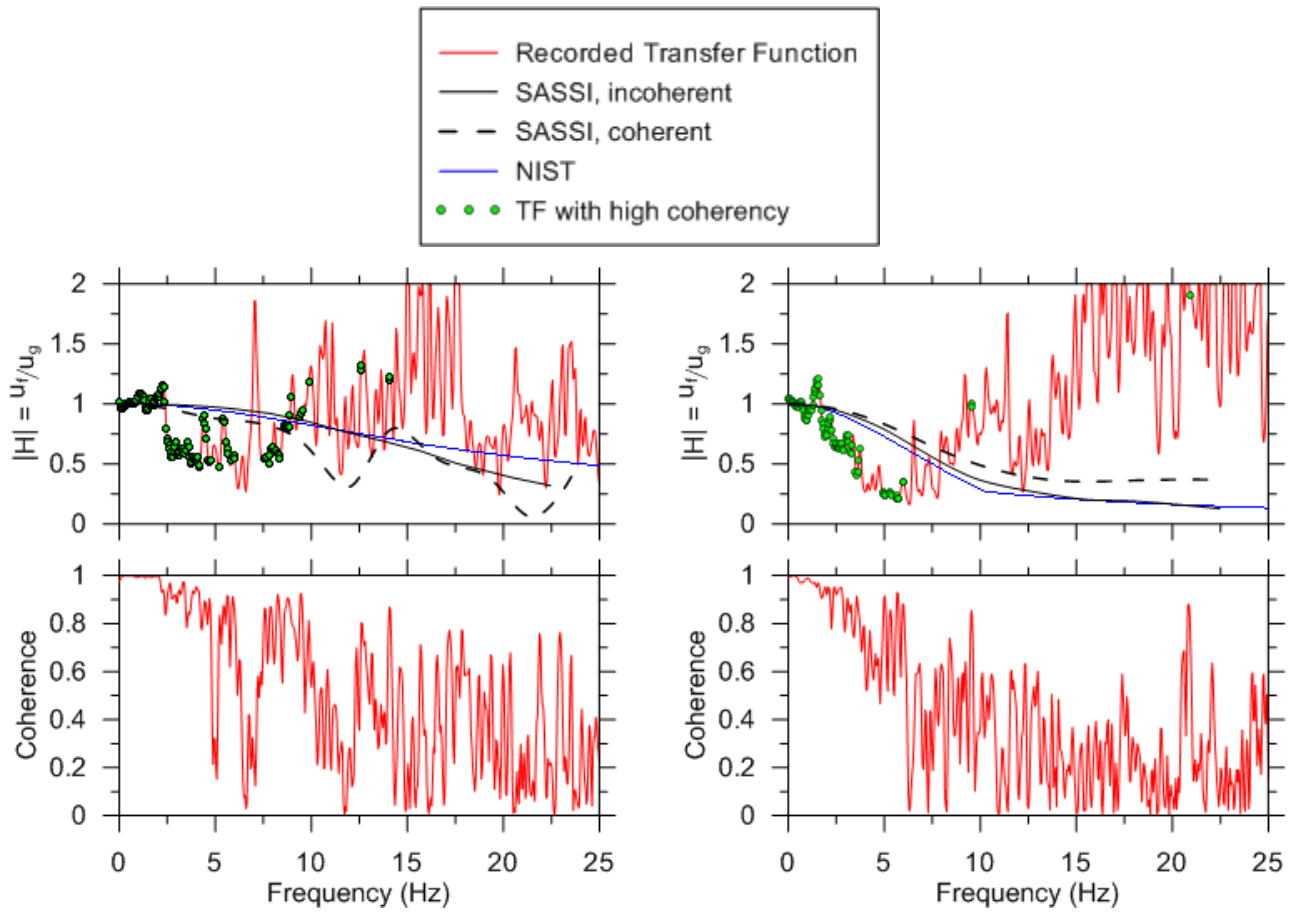


Figure 4. Sendai site horizontal transfer functions and coherence for the 2003 Off Miyagi earthquake.

Figure 6. Onagawa site horizontal transfer functions and coherence for the 2011 Tohoku earthquake.

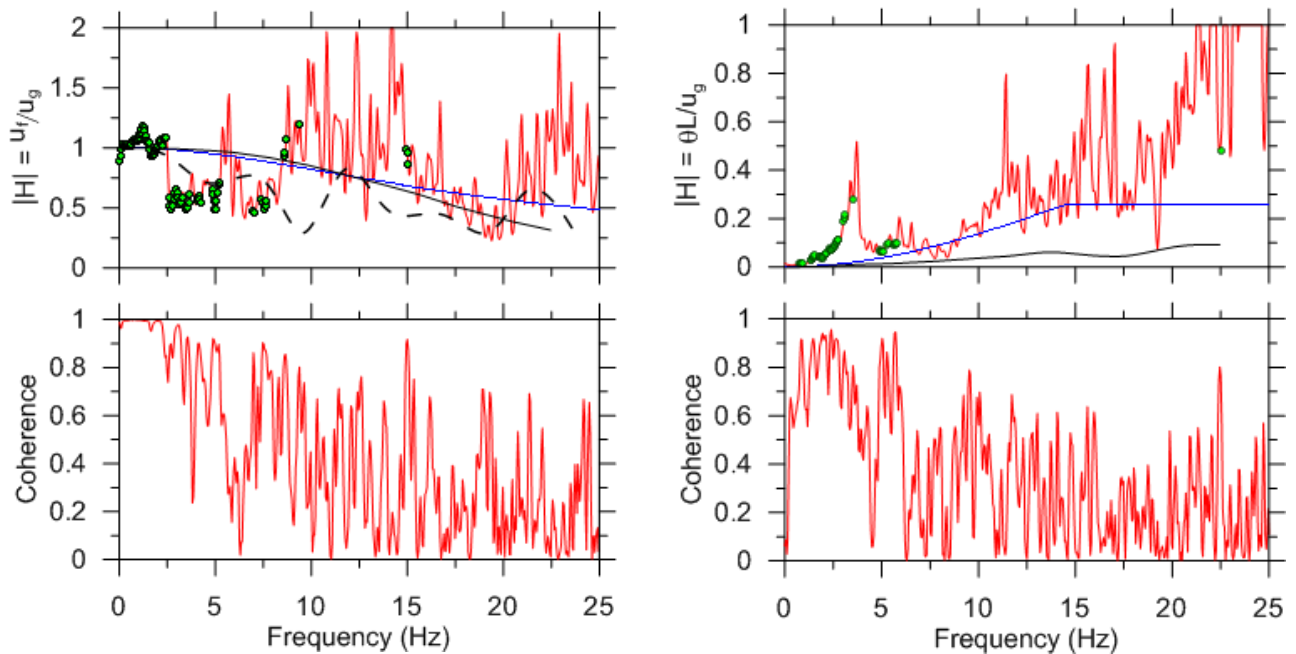


Figure 5. Sendai site horizontal transfer functions and coherence for the 2011 Tohoku earthquake.

Figure 7. Onagawa site rocking transfer functions and coherence for the 2011 Tohoku earthquake.

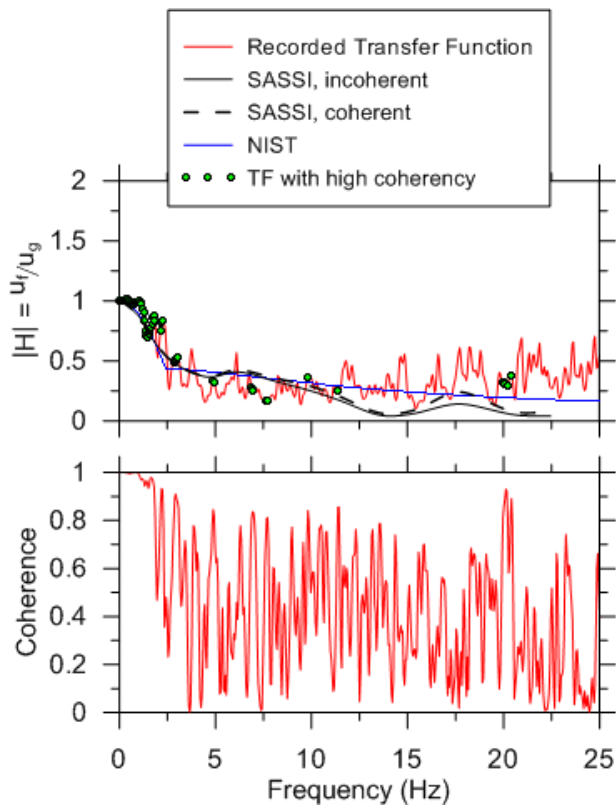


Figure 8. Nagoya site horizontal transfer functions and coherence for the 2004 Off Kii Peninsula earthquake.

In Figures 4-5 at frequencies above about 9 Hz, the coherence is low, being near the range of 0.2-0.3 that is associated with pure noise for the level of smoothing used in the calculations. Some peculiar transfer function ordinates are observed in this range, including transfer function ordinates above unity, but those results are not considered reliable due to the strong effects of noise. Investigation of piles with incoherent inputs is beyond the ability of SASSI. The Sendai building was modeled with piles for the coherent case, however, excluded for the incoherent case.

Figures 6-7 presents horizontal and rotational transfer functions from the Onagawa site. The two models produce similar transfer functions for the horizontal direction. The SASSI model produces higher rotational transfer functions than NIST, which is likely due to stiffer materials below the foundation that are accounted for in the SASSI model. The horizontal transfer functions (Figure 6) from these models over-predict those from data for frequencies under about 7 Hz, where the coherence is sufficiently high for the results to be meaningful. The rotational transfer functions (Figure 7) begin at zero, gradually rise up to about 15 Hz, but have a pronounced peak at about 3 Hz which is likely due to base rocking from inertial interaction. The NIST model matches the data reasonably well whereas the SASSI model under-predicts.

Figure 8 presents horizontal transfer functions for the Nagoya site, which is of special interest because of the large embedment and the relatively large foundation horizontal dimensions, which are near the limit of the calibration range in

the Kim and Stewart study. The data from this site are a relatively high quality as indicated by high coherence over a wide frequency range. The data are quite consistent with the model, and the low transfer function ordinates (indicating substantial reductions of foundation motions relative to free-field motions) are dominated by embedment effects.

## 5. INTERPRETATION AND CONCLUSIONS

It has become increasingly common in recent years for structural engineers to take advantage of kinematic interaction effects to reduce foundation level ground motions relative to those specified in the free-field. The guidelines that appear in NIST (NEHRP CJV, 2012) and other documents account for the effects of base slab averaging and embedment. The base slab averaging model is semi-empirical, being based on a theoretical formulation calibrated for use in California.

We examine data from several sites in Japan to investigate the effectiveness of the NIST procedures, both relative to the data and relative to predictions from the finite element code SASSI. For all three sites, predictions of horizontal transfer functions from the SASSI code and the NIST procedures are similar over the frequency range of principal interest (up to about 10 Hz). For horizontal motions, the model-based transfer functions were too large (hence conservative) for the Sendai and Onagawa sites. For kinematic base rocking, the model-based predictions are accurate from the NIST model but too low from the SASSI model, when compared to data. The model predictions are fairly accurate relative to data at the Nagoya site, which is dominated by embedment effects.

An interesting aspect of the data from the Sendai site is that it has experienced numerous earthquakes of varying shaking amplitudes. Two earthquakes producing moderate and very strong shaking are considered here, with remarkably similar results, suggesting a lack of significant nonlinear effects on the kinematic ground motion reductions for this site. Whether this finding is repeatable and transferable to other sites requires further investigation.

Based on this work, we find generally satisfactory performance of the simplified models for kinematic interaction presented in NIST (NEHRP CJV, 2012) using these data from Japan.

### Acknowledgements:

The authors thank the Tohoku Electric Power Company for providing nuclear power station data and to emeritus Professor Makoto Kamiyama who provided data for site J1.

### References:

- Abrahamson, NA, 1991. Spatial variation of strong ground motion for use in soil-structure interaction analysis, *Proceedings of Fourth U.S. National Conference on Earthquake Engineering*, Vol.1, 317-326.
- American Society of Civil Engineers, ASCE, 2006. Seismic rehabilitation of existing buildings, *Report ASCE/SEI 41-06*, Reston, VA.

- Ancheta, TD, JP Stewart, and NA Abramhamson, 2011. Engineering characterization of earthquake ground motion coherency and amplitude variability, *Proc. 4th International Symposium on Effects of Surface Geology on Seismic Motion*, IASPEI/IAEE, August 23–26, 2011, University of California, Santa Barbara.
- Chubu Regional Bureau office, MLIT, 2003. PS logging at Nagoya Courthouse building complex, unpublished report (in Japanese).
- Chubu Regional Bureau office, MLIT, personal communication 2005. Portions of construction drawings and the soil investigation (in Japanese).
- Darendeli, M 2001. Development of a new family of normalized modulus reduction and material damping curves, *Ph.D. Dissertation*, Univ. of Texas at Austin.
- Ghiocel, DM, 2006. ACS SASSI Version 2.3 – An advanced computational software for system analysis for soil-structure interaction; User manual, *Technical Report*, Rochester, New York.
- Idriss, IM, and JI Sun, 1991. User's manual for SHAKE91: A computer program for conducting equivalent linear seismic response analyses of horizontally layered soil deposits, *Center for Geotechnical Modeling*, Univ. of California, Davis.
- Kausel E, A Whitman, J Murray, and F Elsabee, 1978. The spring method for embedded foundations, *Nuclear Engrg. and Design*, 48, 377-392.
- Kim S and JP Stewart, 2003. Kinematic soil-structure interaction from strong motion recordings, *Journal of Geotechnical and Geoenvironmental Engineering*, ASCE, 129(4), 323-335.
- Lysmer, J, M Tabatabaie-Raissi, F Tajirian, S Vahdani, and F Ostadan, 1981. SASSI – A system for analysis of soil-structure interaction, *Report No. UCB/GT/81-02*, Geotechnical Engineering, University of California, Berkeley.
- Lysmer, J, F Ostadan and C Chin, 1999. *SASSI2000 Theoretical Manual*, Geotechnical Engineering Division, Civil Engineering Department, University of California, Berkeley.
- Menq, FY, 2003. Dynamic properties of sandy and gravelly soils, *Ph.D. Dissertation*, Univ. of Texas at Austin.
- Mikami, A, JP Stewart, F Ostadan, and CB Crouse, 2006. Representation of ground motion incoherence for the analysis of kinematic soil-structure interaction, *Proc. 8<sup>th</sup> U.S. Nat. Conf. Eqk. Engrg.*, April 18-22, San Francisco, CA, Paper 1071.
- Mikami, A, JP Stewart, and M Kamiyama, M., 2008. Effects of time series analysis protocols on transfer functions calculated from earthquake accelerograms, *Soil Dyn. and Eqk. Engrg.*, 28, 695-706.
- NEHRP Consultants Joint Venture, 2012. Soil-Structure Interaction for Building Structures, *Report NIST/GCR 11-917-14*, National Institute of Standards and Technology, Washington, D.C.
- Ostadan, F, 2005. Soil-structure interaction analysis including ground motion incoherency effects, *18th International Conference on Structural Mechanics in Reactor Technology (SMiRT 18)*, Beijing, China.
- OYO Corporation, 2007. PS logging at Tokoku Institute of Technology campus in 2007, unpublished report, September 2007 (in Japanese).
- Tohoku Electric Power Company, 2009. Seismic analysis of Onagawa NPS#1, Siryo 2-1 report (in Japanese).
- Tohoku Electric Power Company, 2009. Vibration characteristics of the ground site, Siryo 2-3 report (in Japanese).
- Tohoku Electric Power Company, 2011. Accelerograms observed at Onagawa NPS during 2011 Great East Japan Earthquake, available on CD-ROM from Japan Association for Earthquake Engineering.
- Veletsos, AS and AM Prasad, 1989. Seismic interaction of structures and soils: Stochastic approach, *J. Struct. Engrg.*, 115 (4), 935–956.
- Veletsos, AS, AM Prasad, and WH Wu, 1997. Transfer functions for rigid rectangular foundations, *J. Eqk. Engrg. Struct. Dyn.*, 26 (1), 5-17.
- Zerva, A and V Zervas, 2002. Spatial variations of seismic ground motion – an overview. *Applied Mechanics Reviews*, 55, 271-297.